THE PROTEOLYSIS OF APOLIPOPROTEIN E IN ALZHEIMER'S DISEASE

by

Julia Love

A thesis

submitted in partial fulfillment

of the requirements for the degree of

Master of Science in Biology

Boise State University

August 2016

BOISE STATE UNIVERSITY GRADUATE COLLEGE

DEFENSE COMMITTEE AND FINAL READING APPROVALS

of the thesis submitted by

Julia Love

Thesis Title: The Proteolysis of Apolipoprotein E in Alzheimer's Disease

Date of Final Oral Examination: 26 April 2016

The following individuals read and discussed the thesis submitted by student Julia Love, and they evaluated her presentation and response to questions during the final oral examination. They found that the student passed the final oral examination.

Troy Rohn, Ph.D.	Chair, Supervisory Committee
Kenneth A. Cornell, Ph.D.	Member, Supervisory Committee
Juliette Tinker, Ph.D.	Member, Supervisory Committee

The final reading approval of the thesis was granted by Troy Rohn, Ph.D., Chair of the Supervisory Committee. The thesis was approved for the Graduate College by Jodi Chilson, M.F.A., Coordinator of Theses and Dissertations.

DEDICATION

This thesis is dedicated to my parents Paul and Cynthia Love, my brother Philip

Love, and all of my friends who have supported and encouraged me along the way.

ACKNOWLEDGEMENTS

There have been many people who have contributed to this work and my academic growth over the course of pursuing my Master's degree. These individual contributions have not gone unnoticed and are an important part of my thesis work. First and foremost, I would like to thank Dr. Troy Rohn for being available with a willing attitude whenever I needed assistance, for his steadfast support and care, and for providing me with every opportunity to exceed what I thought were my limitations. In addition, I appreciate the time and effort he has put forth in helping me write and submit several publications. I would like to thank my committee members Dr. Kenneth Cornell and Dr. Juliette Tinker for their support and helpful suggestions throughout my time here at Boise State University.

I would like to thank my fellow lab members Ryan Day, Collin Wheeler, and Dustin Theis for their availability and help carrying out the experiments in this thesis. I would like to thank my professors, especially Dr. Eric Hayden and Dr. Kristen Mitchell, for their support in the classroom, and in the next steps of my graduate career.

ABSTRACT

Harboring the apolipoprotein E4 (*APOE4*) allele is the greatest genetic risk factor associated with late-onset (sporadic) Alzheimer's disease (AD), however the mechanism by which apoE4 contributes to the pathology of AD is unknown. The proteolysis of apoE4 has been suggested to contribute to AD pathology due to a possible toxic gain, or loss of function. In order to determine if apoE4 is being cleaved, we designed and characterized a site-directed cleavage antibody directed at position D151 of full length human apoE4. The antibody (nApoECFp17) detected a predicted ~17 kDa fragment following incubation with the proteases Type-1 collagenase, and matrix metalloproteinase (MMP)-1and 9. Once the nApoECFp17 amino-terminal antibody was applied to frontal cortex AD brain sections, it revealed nuclear labeling of glial cells and neurofibrillary tangles (NFTs). In addition, nApoECFp17 regionally localized with the protease MMP-9 in plaque-rich regions *in vivo,* suggesting apoE4 may be cleaved extracellularly. Together these data suggest a novel cleavage event of apoE4 by Type-I collagenase and MMP-1 and 9, generating an amino-terminal fragment that is then taken up by glial cells and localizes to the nucleus. This fragment localizing to the nucleus purposes a new role of apoE4 in AD pathology where apoE may alter gene expression.

TABLE OF CONTENTS

LIST OF TABLES

LIST OF FIGURES

LIST OF ABBREVIATIONS

AD	Alzheimer's disease
Aβ	Beta amyloid
NFT	Neurofibrillary tangles
ApoE	Apolipoprotein E
APOE4	Apolipoprotein E4 allele
APP	Amyloid precursor protein
PSEN 1/2	Presenilin 1/2
PHF	Paired helical filament
MAP	Microtubule associated protein
MMP	Matrix metalloproteinases
kDa	Kilo Dalton
His	Histidine
LDL	Low-density lipoprotein
NMDA	N-methyl-D-aspartate
nApoECFp17	N-terminal ApoE cleavage fragment 17 kDa
TTBS	Tween Tris Buffered Saline
EDTA	Ethylenediamine tetra-acetic acid
TBS	Tris buffered saline
GFAP	Glial Fibrillary Acidic Protein

INTRODUCTION

Although the first case of Alzheimer's disease (AD) was described more than 100 years ago, there is still no cure or any effective treatments for this disease. It is known that AD is pathologically characterized by the presence of beta amyloid plaques (Aβ-plaques) and neurofibrillary tangles (NFTs). Current dogma suggests that Aβ formation precedes the formation of NFTs and collectively has become known as the Amyloid Cascade Hypothesis. Current AD research is focused on either targeting the initial formation of Aβ-plaques, and/or how Aβ-plaques and NFTs cause their toxic effects in the brain. The focus of my thesis investigates the role of apolipoprotein E (apoE) proteolysis in promoting AD pathology. The proteolysis of apoE may drive AD pathology by either gaining a new toxic function, losing its normal function, or both. Due to the possible loss and/or gain of function following proteolysis of apoE, the research conducted in this work focuses on apoE's production of a toxic fragment that may influence NFT and Aβ-plaque formation.

The Brain

The brain is a very complex organ both in structure and function in the human body. The brain connects us with our world by allowing us to interact with sensory stimuli. It is vital in connecting us with one another by processing language and emotion. Most importantly, the cerebral cortex of the brain is responsible for many of the higher executive functions that contribute to distinguishing humans from other species. The

brain is a very powerful organ of which we have only scratched the surface in discovering its true capabilities.

The human central nervous system consists of the brain and spinal cord. Through a network of nerve cells and connections, information from the central nervous system is distributed throughout the body. The brain is composed of grey matter (cell bodies, dendrites, and axon terminals of neurons) and white matter (axons that connect parts of the grey matter together), which is encased in a bony structure called the cranium. The brain consists of two cell types, neurons and glial cells. Neurons are specialized cells that transmit nerve impulses, and are the fundamental units of the nervous system. The structure of a neuron consists of a central cell body housing the nucleus, an axon for signal transduction, and dendrites for receiving information. The brain is composed of roughly 100 billion neurons, however, there are 10-50 times that number of glial cells in the human brain. Unlike the communication functionality of neurons, glial cell function is to protect and support neurons. Glial cells provide oxygen, insulation, hold neurons in place, and clean up cellular debris. There are three types of glial cells; 1) astrocytes, which are star-like cells that link neurons to blood vessels 2) oligodendrocytes, which support and insulate axons and 3) microglia, which are systemically analogous to white blood cells.

Alzheimer's Disease

Alzheimer's disease (AD) is a progressive, irreversible neurodegenerative disease characterized by neuronal death and synaptic pruning [1]. AD is the most common form of dementia and results in memory deficits, language difficulties, impairment of visuospatial abilities, as well as other cognitive impairments [2]. Currently, AD affects

over 5 million people in the United States alone and annually costs the national healthcare system over 243 billion dollars. The high cost to care for those afflicted with AD emphasizes the importance of discovering preventative strategies, and effective treatments in hopes of a cure.

Currently, the mechanisms associated with AD pathology are unclear. However, the involvement of Aβ plaques appear to be central in leading to neuronal degeneration. Aβ plaques are insoluble aggregates of the amyloid β peptide that collect in the brain parenchyma surrounding neurons and glial cells. Production of Aβ results from the proteolysis of the amyloid precursor protein (APP) by either α, β, or γ secretases [3]. The β secretase cleaves APP, resulting in a soluble amino terminal fragment containing extracellular sequences of APP. However, cleavage of APP by the α secretase results in a soluble amino terminal fragment, as well as a carboxyl-terminal membrane bound fragment. The γ secretase can further cleave the membrane-bound carboxyl-terminal fragment or the amino-terminal fragments producing Aβ. The increase in Aβ leads to induction of oxidative stress, apoptosis, and disrupted axonal transport, ultimately resulting in defective cognitive ability and NFT pathology [3].

Research suggests the protein tau contributes to NFT formation in AD. Tau is a microtubule associated protein (MAP) and is expressed in the neuronal axon. Tau normally functions to stabilize the cytoskeleton by binding to microtubules and also plays a role in anterograde transport in neurons and glial cells. Tau can be hyperphosphorylated resulting in a decreased binding affinity to microtubules and subsequent aggregation of tau into beta sheet structures termed paired helical filaments (PHFs), which then aggregate as rope-like structures composed of two fibers twisted around one another [4].

The loss of function of tau in AD decreases the ability of microtubules to bind to tubulin for proper assembly and polymerization, increasing the occurrence of aggregating tau binding to normal tau [5].

Alzheimer's Disease Diagnosis and Treatment Strategies

Clinical diagnosis of AD is primarily made by exclusion of other causes of dementia. A true diagnosis of AD can only be obtained by performing an autopsy with post mortem tissue analysis [6]. Thus, there is a demand for biomarkers associated with AD, not only for proper diagnosis, but also to determine susceptibility to AD and to assess treatment strategies. Currently, there are no prevention measures that can be taken for AD. Drugs on the market to aid with AD treatment are designed to maintain synapses and overall neuron function. Examples of AD drug targets are: the hyperphosphorylation of tau, NMDA receptor blockade, acetylcholinesterase inhibition or nicotinic receptor agonists, and neurotransmitter balance [7]. Aside from the therapeutic approach to help control symptoms of AD, disease modifying strategies are also under investigation aimed at reducing Aβ levels in the brain and reestablishing tau function. In order to achieve this goal, current gene therapy techniques such as lentiviruses or viral vectors are becoming more popular [8], as well as cell replacement therapies [9]. Very new on the horizon is analyzing the epigenetic component of AD, which could be useful for determining biomarkers and predisposition [10].

Risk Factors in Alzheimer's Disease

The greatest risk factor for AD is advancing age with current statistics indicating that 11 percent of those age 65 and older and 32 percent of people age 85 and older are afflicted with this disease [11]. There are two types of AD: early-onset familial AD

(before age 65) and late-onset or sporadic AD. Early-onset AD is caused by mutations in the amyloid precursor protein (*APP*) or presenilin-1 (*PSEN 1*) and presenilin-2 (*PSEN 2*) genes. Mutations in these proteins ultimately enhance production of Aβ, which leads to an increase in Aβ-plaque deposition. Additionally, the increase in plaque formation could be due to a failure to remove or clear Aβ from the brain, contributing to AD pathogenesis.

Several genetic risk factors are also associated with late-onset AD such as *A2M* (encoding alpha-2-macroglobulin), *ABCA1* and *2* (encoding ATP-binding cassette transporters 1 and 2, respectively), *CLU* (encoding clusterin), *PICALM* (encoding the phosphatidylinositol binding clathrin assembly protein) and *SORL1* (encoding sortilin-related receptor gene) *TREM2*, and *APOE4*. There are two variants of *TREM2* that increase the risk of AD by three fold by either stimulating phagocytic activity or by decreasing microglial pro-inflammatory responses [12]. However, the greatest genetic risk factor is harboring the apolipoprotein E4 (*APOE4*) allele. The inheritance of one copy of *APOE4* increases the risk of AD four fold, while inheritance of two copies raises the risk about tenfold. Despite the well-known risk associated with inheritance of the *APOE4* allele, the mechanism by which the apoE4 protein contributes to AD pathology has not been definitively established.

APOE Structure and Function

Human apoE is polymorphic with three major isoforms, apoE2, apoE3, and apoE4, which differ by a single amino acid substitution involving cysteine-arginine replacements at positions 112 and 158 [13]. Harboring the *APOE3* allele is believed to neither increase nor decrease one's risk of AD, having the *E2* form may actually decrease one's risk, while having the *E4* allele increases risk. Structurally, apoE4 is a 34 kDa

protein composed of 299 amino acids and contains two major domains, referred to as the *N*-terminal and *C*-terminal domains, which are connected by a short-hinge region [14] . ApoE is expressed by astrocytes, some microglia, and in certain circumstances neurons [15]. In the CNS, apoE functions to transport cholesterol to neurons through binding and uptake by apoE low density lipoprotein (LDL) receptors [16]. Cholesterol released from apoE-containing lipoprotein particles is used to support synaptogenesis and the maintenance of synaptic connections [17]. Differences among apoE isoforms in these processes may negatively impact synaptic plasticity or recovery of neurons from neurodegeneration as might occur in AD [18].

Proteolysis of APOE

ApoE4 plays a normal role in lipoprotein transport in the brain, however the mechanism by which apoE4 contributes to AD pathogenesis remains elusive. It has been hypothesized that apoE4 is much more susceptible to proteolysis than the E2 or E3 form due to the numerous proteolytic cleavage sites in the hinge region of apoE4 [19]. Although the hinge region is particularly susceptible to proteolysis, there is evidence to support other susceptible regions of apoE4 such as the N-terminal and C-terminal domains [20]. In mouse models, production of apoE by neurons is associated with apoE fragmentation, whereas production of apoE by astrocytes is not [19]. Neuronal proteolysis of apoE4 occurs preferentially in regions of the brain that are susceptible to AD and neurodegeneration [21]. Additionally, proteolysis of apoE4 occurs to a greater extent than for apoE3, and is associated with enhanced phosphorylation of tau [21]. There are several studies that have demonstrated the presence of fragmented apoE4 in the AD

brain [19, 21, 22], supporting the hypothesis that the proteolysis of apoE4 could contribute to neuropathology and neurodegeneration in AD.

When apoE4 is cleaved, two distinct domains are produced and each are associated with a specific pathological structure in the AD brain; the C-terminal domain of apoE4 binds to beta amyloid and primarily localizes to plaques [22, 23], while the N-terminal domain mainly localizes to NFTs [19]. ApoE4 fragments produced by proteolytic cleavage have been found to be associated with either a toxic gain of function or a loss of normal function. Altered function of apoE4 due to the high susceptibility of apoE4 to proteolysis may be responsible for the heightened risk associated with inheritance of the *APOE4* allele.

APOE Proteolysis Leads to a Loss of Function

The main function for apoE in the CNS is to transport cholesterol. As mentioned previously, proteolysis of apoE occurs in neurons, not in astrocytes. In normal conditions, neurons express very little apoE. However, expression of apoE is increased in neurons under circumstances requiring neuronal repair, remodeling, and response to injury [24, 25]. ApoE may be providing the necessary cholesterol for neuronal repair as well as synapse formation, plasticity, and repair [26]. The efficiency of apoE4 to transport cholesterol and maintain neurons in response to injury may be reduced when compared with the E2 and E3 isoforms and this could be due to lower levels of the apoE protein in the brain following proteolysis of the protein [27].

In addition to the role of apoE in cholesterol transport, apoE also plays a role in the clearance of Aβ deposition in the AD brain. It is hypothesized that apoE binds to Aβ and induces a pathological β-sheet conformational change in Aβ [28]. Studies have

reported that apoE3 and E2 form more stable complexes with Aβ and to a much greater extent than E4 [29], and therefore, the better binding efficiency of apoE3 and E2 may enhance Aβ clearance compared with apoE4 [30]. In a recent study, an AD mouse model crossed with mice expressing C-terminal-truncated apoE4 showed these mice had a lower affinity for beta amyloid and reduced ability to clear beta amyloid [31]. Additionally, the *APOE* allele dosage is associated with increased plaque deposits in AD [32]. In a large cerebrospinal fluid (CSF) study of cognitively normal middle-aged people ("at risk" for AD), Aβ deposition was associated with low CSF levels of Aβ42 [34]. In carriers of the *APOE4* allele, lower CFS levels of Aβ42 were observed, emphasizing analysis of CSF levels as pre-clinical detection tool for tracking of AD in "at risk" individuals [33].

APOE Proteolysis Leads to a Toxic Gain of Function

The proteolytic cleavage of apoE4 not only may lead to a loss of function, but it may also produce a toxic-gain of function. The cleavage of apoE4 produces N- and C-terminal fragments that are neurotoxic in nature [22, 34, 35]. It has been hypothesized that these fragments are generated following intraneuronal processing of apoE4 [22]. The N-terminal fragment containing the receptor binding region of apoE4 (1-191) is responsible for binding with tau [36] as well as the hyperphosphorylation of tau, a key step in the evolution of NFTs [21]. The neurotoxicity of N-terminal fragments may also promote the underlying pathology of AD by producing tangle-like inclusions, which are similar to early NFTs both *in vitro* and in animal models [19, 34, 35]. The C-terminal fragment containing the lipid- binding region (171-272) of apoE4 interacts with mitochondria and C-terminal fragments have been shown to impair function and integrity of mitochondria [34]. In addition, apoE4 fragments may lead to mitochondrial

dysfunction by binding to mitochondrial proteins and enzymes and altering their activities [37]. Another possible toxic gain of function involves oxidative stress. In this regard, a specific fragment of apoE4 promotes cellular uptake of extracellular Aβ leading to the formation of reactive oxygen species [38]. Finally, in a transgenic AD mouse model, expression of a C-terminal-truncated fragment of apoE4 resulted in behavioral deficits and a failure to clear Aβ deposition [31]. These results support the notion that fragments produced from the proteolysis of apoE4 gain a toxic function and enhance the underlying pathological mechanisms of AD.

Hypothesis

The exact nature of the protease involved in cleaving apoE4 is unknown although several candidate proteases have been reported including cathepsin D [39], a chymotrypsin-like protease [19], aspartic proteases [40], and caspases [23]. Previous studies on the proteolysis of apoE4 in AD have identified the presence of a ~18 kDa band in the human AD brain extracts, suggesting cleavage near position D154 of the mature form of apoE4 (299 amino acids) [19, 22]. This site was chosen based on it being a putative caspase consensus cleavage site. Rohn et al. synthesized and characterized a site-directed cleavage antibody aimed at specifically recognizing this ~18 kDa fragment of apoE4 found in AD samples. However, results indicated a protease other than caspase was cleaving apoE4 at this site. Therefore, examination of an additional caspase-cleavage consensus site with apoE4 was undertaken that would produce a slightly smaller amino-terminal fragment (~17 kDa) following putative cleavage of apoE4 by caspase-3 [23]. Thus, an additional site-directed antibody was designed to target position D151 just

upstream of D154 [23], which will be referred to as nApoECFp17 for the duration of this work.

Matrix metalloproteinases (MMPs) are a family of calcium-requiring and zinc-containing endopeptidases and evidence has suggested that MMPs may play an important role in the pathogenesis of AD [41]. Type IV collagenase or MMP-9 is a major MMP that is expressed and released by neurons, microglia, and astrocytes [42]. MMP-9 has also been identified in neuroinflammation [42]. ApoE4 has been previously associated with brain inflammation and AD patients with the *E4* allele show increased microglial activation compared with AD patients not carrying the E4 allele [43]. In a study conducted by Dafinis et al., a particular apoE4 fragment lead to increased extracellular levels of MMP-9 [38]. The hypothesis tested in my thesis is that full length apoE4 is a target for proteolytic cleavage by MMP-9, resulting in a predicted ~17 kDa fragment and this fragment is present in the AD brain.

METHODS

Materials

Human recombinant apoE4 and E3 proteins purified from *E. coli* were purchased from ProSci Inc. (Poway, CA). Activated human recombinant caspase-3 was purchased from Calbiochem (San Diego, CA). The anti-apoE4 N-terminal full-length rabbit polyclonal antibody was purchased from Aviva Systems Biology Corp. (San Diego, CA). PHF-1 was a generous gift from Dr. Peter Davies (Albert Einstein College of Medicine, Bronx, NY). Type I collagenase was from Sigma-Aldrich (St. Louis, MO) and purified collagenase was from Worthington Biochemical (Lakewood, NJ). Active MMP-1 and the mouse monoclonal MMP-9 antibody were purchased from Abcam Inc. (Cambridge, MA), while active MMP-9 was purchased from EMD Millipore (Billerica, MA). The monoclonal antibodies, Olig-1 and Iba1/AFI1, were purchased from EMD Millipore (Billerica, MA).

Generation of the Polyclonal Site-Directed Cleavage Antibody to ApoE4

Synthesis of polyclonal antibodies was accomplished using the 7-mer peptide C-RKRLLRD, which represents the N-terminal upstream neoepitope fragment of apoE4 generated following cleavage after the aspartic acid residue located at position D151 of the mature form of apoE4. Following synthesis, this peptide was coupled to KLH and injected into two rabbits. The resulting sera (verified by ELISAs, Fig. 2) were used to affinity purify antibodies using a Sulfolink™ column (Thermo Scientific) coupled with the peptide used as an immunogen. For this antibody, synthesis of peptides, injections of

immunogens, and collection of antisera were contracted out to Bethyl laboratories (Montgomery, TX).

ELISA

To verify the polyclonal site-directed cleavage antibody, 40µl of the N-terminal neopeptide fragment of apoE4 following cleavage at position D151 was mixed with coating buffer and added to 32 wells of a Dynex plate, covered, and incubated overnight on a rocker at 4°C. TTBS (pH 7.5) was used to wash the plate after each incubation. 300 µl of blocking buffer was added to each well and was covered to incubate for 1 hour at 37° C. Dilutions of the pre-immunized and immunized sera ranged from 1:250- 1:32000. The 1:250 dilution contained 4 µl of either pre-immunized or immunized serum and 996 µl of diluting buffer. Serial dilution was carried out until the 1:32000 dilution. After the blocking stage, each dilution was added to the corresponding well and incubated for 2 hours at 37°C. The secondary antibody was a 1:5000 dilution of horseradish peroxidase (HRP). The plate was washed and 100 µl of the secondary solution was added to each well to incubate for 1 hour at 37°C. The plate was washed and 100 µl of TMB Microwell Peroxidase substrate was added to each well. After 4 minutes, 100 µl TMB Stop solution was added to each well. The plate was then read at a wavelength of 450 nm.

Cell-free assays/Western Blots

For the proteolysis of apoE4, 40 µg of purified human recombinant apoE4 was incubated with active human recombinant caspase-3 at 37° C overnight in 2x reaction buffer containing 10 mM DTT. Type I collagenase, purified collagenase, MMP-1, and 9 experiments were carried out utilizing a reaction buffer containing 100 mM Tris-HCL, 10

mM CaCl$_2$, pH 7.8. The reactions were terminated by adding 5x sample buffer and were stored at -20° C.

For Western blot analysis, samples were separated by 15% SDS PAGE (sodium dodecyl sulfate polyacrylamide gel electrophoresis) and transferred to nitrocellulose. Transferred gel slabs were stained in Coomassie blue to verify equal loading between samples. Nitrocellulose membranes were incubated in nApoE4CF antibody (1:500) overnight at 4°C and primary antibodies were visualized using goat anti-rabbit HRP-linked secondary antibody, incubated for 1 hour at room temperature (1:5,000; Jackson's Laboratory, West Grove, PA), followed by ECL detection.

Immunoprecipitation and Mass Spectrometry

Immunoprecipitation experiments were conducted by incubating the nApoECFp17 antibody with apoE4 samples digested with Type I collagenase. To terminate the actions of Type I collagenase, 100 mM EDTA (ethylenediamine tetra-acetic acid) was added at the conclusion of the experiment. Samples were incubated overnight at 4°C with nApoECFp17 antibody and then 50 µl of Protein A agarose beads were added for 2 hours at 4°C. The agarose beads were then spun down and washed 3X in PBS. Samples were prepared for Western blot analysis as described above utilizing a commercial antibody that recognizes the extreme amino-terminus of full-length apoE4.

For mass spectrometry experiment samples were separated by 15% SDS PAGE and gel slices were excised from SDS-PAGE gels and digested with trypsin. Briefly, excised bands were destained in 25 mM ammonium bicarbonate/50% acetonitrile overnight at 4°C. Gel slices were dehydrated in 100% acetonitrile for 10 minutes at room temperature, followed by reduction in 10 mM DTT for 60 minutes at 37°C. Next,

alkylation was performed in 55 mM iodoacetamide for 60 minutes at room temperature in the dark. Protein samples were digested with trypsin in 10 mM ammonium bicarbonate overnight at 30°C. Digested peptides were separated using reversed phase chromatography (Thermo Scientific Easy-nLC II) and infused into a Velos Pro Dual-Pressure Linear Ion Trap Mass Spectrometer for MS/MS using CID fragmentation. Results were analyzed with Thermo Scientific's Proteome Discoverer software (v1.3) and the Mascot search engine probing the human SwissProt database. Search parameters included carbamidomethyl (C) fixed modification, oxidation (M) variable modification, maximum of 2 missed cleavages, and 1.5 Da peptide mass tolerance.

Human Subjects

Autopsy brain tissue from the frontal cortex of nine neuropathologically confirmed AD cases with known apoE isoform genotype and three age-matched control cases were studied. Fixed frontal cortex tissue sections used in this study were provided by the Institute for Memory Impairments and Neurological Disorders at the University of California, Irvine. Approval from Boise State University Institutional Review Board was not obtained due to the exemption granted that all tissue sections were fixed and received from University of California, Irvine. Brain tissue obtained from University of California, Irvine were anonymized and never identified except by case number. Tissue donors or their next of kin provided signed informed consents to the Institute for Memory Impairments and Neurological Disorders for the use of their tissues in research (IRB 2014–1526). Case demographics are presented in **Table 1**.

Immunohistochemistry

Free-floating 40 μm-thick serial sections were used for immunohistochemistry and immunofluorescence as previously described above. For bright-field labeling, sections were washed with 0.1 M Tris-buffered saline (TBS), pH 7.4, and then pretreated with 3% hydrogen peroxide in 10% methanol to block endogenous peroxidase activity. Sections were subsequently washed in TBS with 0.1% Triton X-100 (TBS-A) and then blocked for thirty minutes in TBS-A with 3% bovine serum albumin (TBS-B). Sections were further incubated overnight at room temperature with the antibodies at the described concentrations above. Following two washes with TBS-A and a wash in TBS-B, sections were incubated in anti-rabbit or mouse biotinylated anti-IgG (1 hour) and then in avidin biotin complex (1 hour) (ABC, Elite Immunoperoxidase, Vector Laboratories, Burlingame, CA, USA). The primary antibody was visualized using brown DAB substrate (Vector Laboratories).

Immunofluorescence Microscopy

For immunofluorescence co-localization studies, experiments were initiated by incubating in primary antibody overnight followed by application of the ABC, Elite Immunoperoxidase kit on day 2 (Vector Laboratories, Burlingame, CA, USA). In this case, instead of completing the staining use DAB substrate, we employed Alexa fluor 488-labeled tyramide (green, Ex/ Em=495/519) that was purchased as part of the TSA (Tyramide signal amplification) kit #12 (Life technologies, Green Island, NY). Following labeling with the primary antibody, sections were washed 3X in Tris buffer followed by incubations in Tris A (15 minutes) and Tris B (30 minutes). Sections were then incubated with the second primary antibody overnight at room temperature. On day 3, sections were

incubated with secondary biotinylated-SP (long spacer) AffiniPuregoat anti-mouse or rabbit IgG for 1 hour (Jackson Immuno Research Labs (West Grove, PA). This was followed by incubation in streptavidin Alexa Fluor 555 conjugate for 1 hour (Life technologies, Green Island, NY). Following 3X washes in Tris buffer, sections were mounted and cover slipped using Pro-Long Gold Antifade with DAPI (Life technologies). To determine if cross-reactivity to reagents was a factor in double-labeling experiments, experiments were replicated with the antibodies in reverse.

An Olympus BX60 microscope with fluorescence capability equipped with a MagnaFire SP software system for photomicrography was employed for microscopic observation and photomicrography of the diaminobenzidine (DAB)-labeled and fluorescent sections. The fluorescent molecules were excited with a 100-W mercury lamp. Fluorescent-labeled molecules were detected using a filter set having a 460–500-nm wavelength band pass excitation filter, a 505-nm dichroic beam splitter, and a 510–560-nm band pass emission filter.

Confocal Microscopy

For confocal immunofluorescence imaging, the primary antibodies were visualized with secondary antibodies tagged with either Alexa Fluor 488 or Alexa Fluor 555 (Invitrogen, Carlsbad, CA). Images were taken with a Zeiss LSM510 Metasystem combined with the Zeiss Axiovert Observer Z1inverted microscope and ZEN2009 imaging software (Carl Zeiss, Inc., Thornwood, NY). Confocal Z-stack and single plane images were acquired with an Argon (488 nm) and a HeNe (543 nm) laser source. Z-stacks images were acquired using a 20x Plan-Apochromat (NA 0.8) objective, emission band passes of 505–550 nm for the detection of the green channel, Alexa Fluor 488 and

550–600 nm for detection of the red channel, Alexa Fluor 555. All images displayed are 2-D, maximal intensity projections generated acquired Z-stacks. Single plane images were acquired with a 63x Plan-Apochromat oil-immersion objective (NA 1.4) with emission long pass of 505 nm for the detection of the green channel using Alexa Fluor 488 and 550–600 nm for the detection of the red channel using Alexa Fluor 555.

Quantification and Statistical Analysis

Statistical difference between the average number of nApoE4CFp17-positive NFTs in 3 AD cases from each allelic combination of ApoE3/ApoE3, ApoE3/ApoE4, and ApoE4/ApoE4A was determined using Student's two-tailed T-test. To determine the percent co-localization, a semi-quantitative analysis was performed by taking 40X immunofluorescence, overlapping images from three different fields in frontal cortex brain sections of three separate AD cases. Capturing was accomplished by using a 2.5x photo eyepiece and a Sony high resolution CCD (charged-coupled device) video camera (XC-77). As an example, to determine the percent co-localization between Iba-1 and nApoE4CFp17, photographs were analyzed by counting the total number of double-labeled cells per 40X field for each case, and the number of cells labeled with each antibody alone. Statistical differences in this study were determined using Student's two-tailed T-test employing Microsoft Office Excel.

RESULTS

In a previous study, we identified a ~17 kDa band when incubating human

recombinant apoE with activated caspase-3 [23]. Based on results from that study, we

designed a site-directed cleavage antibody based on a caspase-cleavage recognition site at

position D151 (LLRD) of the full-length form of apoE4 that would give a predicted

amino-terminal fragment of ~17 kDa (Fig. 1). Following synthesis of a 7-mer peptide

RKRLLRD, this peptide was coupled to KLH and injected into rabbits. Peptide-specific

anitbodies were affinity purified from resulting sera, which was verified by ELISA (Fig.

2). Western blot analysis was performed to determine if nApoECFp17 could label the

predicted 17 kDa fragment following incubation with caspase-3. Figure 3A shows that

we were unable to detect any band following incubation of full-length apoE4 with

caspase-3. We hypothesized that since apoE4 is a secreted protein, any potential protease

would be located extracellularly, therefore we next tested collagenase. Incubation of

recombinant apoE4 with Type I collagenase generated a ~17 kDa fragment that was

detected by nApoECFp17 (Fig. 3A, second lane, left panel). The nApoECFp17 antibody

did not react with full-length apoE4, nor did the antibody detect any fragments following

incubation with recombinant apoE3 (Fig. 3A, left panel). To confirm the specificity of

nApoECFp17, we preformed immunoprecipitation experiments by incubating

nApoECFp17 with apoE4 that had been digested with Type I collagenase. The

nApoECFp17 antibody immunoprecipitated a ~17 kDa fragment that was detected by

Western blot using an apoE4 antibody whose epitope is at the extreme amino-terminus of

apoE4 (Fig. 3B). Additionally, mass spectrometry of the 17 kDa band indicated 77%

sequence coverage of amino acids 1-151 of apoE4.

The Type I collagenase originally used was a bacterial collagenase preparation

that included collagenase, caseinase, clostripain, and tryptic activities. The experiments

were performed again using purified collagenase as well as MMP-9 and MMP-1 given

that the MMPs have a high degree of homology with collagenase. When apoE4 was

cleaved by purified collagenase, high molecular weight bands were produced that were

detected by nApoECFp17 (Fig. 3C, left panel). These high molecular weight bands

suggest that the cleavage of apoE4 may result in aggregation. Incubation of full-length

apoE4 with MMP-9 produced similar results as Type I collagenase, however, incubation

with MMP-1 produced a high-molecular weight band only when the concentration of

recombinant apoE4 was doubled (Fig. 3C, left panel). These results suggest

nApoECFp17 detects an amino-terminal fragment of apoE of ~17 kDa at the cleavage

site D151, and that MMP-9 can generate this fragment *in vitro*. In addition, Western blot

analysis following incubation of apoE3 with MMP-9 indicated that apoE3 is also

proteolyzed generating in this case only high molecular weight bands (Fig. 5).

To further test the specificity of the nApoECFp17 antibody, an amino-terminal

protein fragment of apoE4 was synthesized corresponding to the predicted length

following cleavage at D151. This amino-terminal fragment (herein termed apoE4$_{1-151}$)

also contained a 6X histidine (His) tag to facilitate purification from *E. coli*. In this

manner, the 6X His tag was attached either at the N-terminal end of apoE4$_{1-151}$ or to the

C-terminal end of apoE4$_{1-151}$. The addition of the His tag to this fragment greatly

influenced whether the nApoECFp17 antibody recognized the fragment. Thus, when the

His tag was attached to the C-terminal end of apoE4$_{1-151}$, there was limited detection by nApoECFp17 in either ELISA assays (Fig. 4A) or Western blot analysis (Fig. 4B). We interpret these data to suggest that the addition of the His tag to the C-terminal end of apoE4$_{1-151}$ prevented the nApoECFp17 from binding to its epitope on the C-terminal end of the fragment. These data further support the specificity of the nApoECF-17 antibody for the C-terminal region of apoE4 following cleavage at D151.

After Western blot analysis confirmed the cleavage of apoE4 *in vitro,* immunohistochemical experiments were done using postmortem frontal cortex brain sections from AD cases. In order to establish the staining profile of nApoECFp17 antibody labeling in AD brain sections, single label, bright-field experiments were carried out. The results indicated immunoreactivity by the nApoECFp17 antibody in all AD cases examined. The strongest labeling was in neurons (Fig. 6A and B), neuropil threads (PHFs with abnormally phosphorylated tau protein) in plaque regions (Fig. 6C), blood vessels (Fig 6D), and small circular structures in gray and white matter (Fig. 6E).

Additional experiments supported the specificity of the nApoECFp17 antibody including a lack of staining observed following application of preimmune serum, and preadsorption of the affinity-purified antibody with the immunogenic peptide, which significantly reduced labeling in serial AD sections (Fig. 7A-D). In addition, there was no staining of the nApoECFp17 antibody in aged matched controls, and when AD cases were compared with normal cases, there was a significant increase in the number of labeled nuclei in AD cases (p=0.0004) (Fig. 7E and F).

Due to the small size of the circular structures, we hypothesized that the labeling was occurring in the nuclei of glia cells. To test the nuclear localization of nApoECFp17

in glia cells, the glial markers Iba-1 (to detect microglia), Olig-1 (to detect oligodendrocytes, and GFAP (Glial fibrillay acidic protein) (to detect astrocytes) were used. In each case, 4'6-diamidino-2-phenylindole (DAPI) was used as the nuclear stain to verify the staining that was being observed was nuclear. In Figure 8 A-D and I, the merge of the staining of Iba-1, DAPI, and nApoECFp17 in representative frontal cortex AD sections indicated approximately 80% of microglia were labeled by nApoECFp17 antibody. Additionally, the merge of Olig-1, DAPI, and nApoECFp17 indicated about 27% of oligodendrocytes were labeled with the nApoECFp17 antibody (Fig. 8 E-H, J). There was no co-localization of nApoECFp17 with GFAP under similar experimental conditions (Fig. 8 K-M).

To confirm whether the amino terminal fragment labeled by nApoECFp17 localizes to NFTs as opposed to plaques, double label experiments were conducted with the two known tangle markers AT8 and PHF-1. The presence of nApoECFp17 was present in fibrillary tangles, a subset of NFTs that were labeled by PHF-1. However, nApoECFp17 also stained neurons that were negative for AT8 or PHF-1 (Fig. 9).

In a final set of experiments, we examined whether nApoECFp17 labeling occurs together with MMP-9, an extracellular protease that was able to generate the predicted ~17 kDa fragment *in vitro* (Fig. 3C). As an initial approach, we screened representative frontal cortex brain sections from AD subjects using bright-field microscopy in single-label experiments utilizing a human anti-MMP-9 monoclonal antibody. The presence of MMP-9 was evident within plaque-rich regions in outer cortical layers and appeared to be extracellular as expected (Fig. 10A and B). Next, double-label confocal immunofluorescence experiments were undertaken using the same MMP-9 antibody

together with nApoECFp17. In this case, although there was no co-localization between the two antibodies, the two markers did occur within close proximity to one another raising the possibility that MMP-9 may cleave apoE4 *in vivo* (Fig. 10C-E).

DISCUSSION

Harboring the *APOE4* allele increases risk for AD, however, despite exhaustive

efforts, the mechanism responsible for enhanced risk of harboring this allele remains

elusive. What separates apoE4 from the other isoforms (E3 and E2) is that apoE4 is more

susceptible to proteolysis and produces fragments that are neurotoxic in nature [19, 34,

35]. In order to identify these fragments in the human AD brain, we designed a site-

directed cleavage antibody targeting position D151 of full-length mature form of human

apoE4. *In vitro*, this antibody, which we have termed the nApoECFp17 antibody,

specifically labels an amino-terminal fragment of apoE4 of the correct predicted

molecular weight of ~17 kDa fragment following cleavage at position D151. Most

importantly, nApoECFp17 does not interact with full-length apoE4 or E3. Generation of

this amino-terminal fragment and recognition by nApoECFp17 was only observed with

recombinant apoE4 and not E3 following digestion with Type I collagenase. In addition,

immunoprecipitation pull-down experiments using the nApoECFp17 antibody revealed a

~17 kDa fragment that was detected by a commercial antibody whose epitope was

located at the extreme amino-terminus of full-length apoE4. Mass spectrometry of the

~17 kDa fragment indicated a 77% sequence coverage of amino acids 1-151 of apoE4.

That the epitope for the nApoCFp17 antibody is at the C-terminal end of this amino-

terminal fragment was confirmed following synthesis of ApoE4 1-151 protein fragments.

A 6X histidine (His) tag was incorporated either at the N- or C-terminal end of $ApoE4_{1-151}$ to facilitate purification from *E. coli*. ELISA and Western blot results indicated that

the nApoECFp17 antibody was only able to recognize ApoE4$_{1\text{-}151}$ in which the His tag was attached to the amino-terminal end. Additional experiments in situ using postmortem frontal cortex brain sections confirmed the specificity of the nApoECFp17 antibody. These immunohistochemical experiments included showing co-localization of nApoECFp17 within NFTs and not plaques. Previous studies emphasize this concept of amino-terminal fragments localizing specifically with NFTs while carboxyl-terminated fragments contribute to AD pathology in aiding in the formation of NFTs, but localize to plaques only [19, 22, 23]. Moreover, labeling by nApoECFp17 was prevented following preadsorption experiments with the peptide corresponding to the upstream sequence (RKRLLRD) that would be generated following cleavage of apoE4 at position D151.

ApoE is primarily synthesized and secreted from astrocytes and microglia [15], but surprisingly, nApoECFp17 strongly labeled nuclei of glial cells as well as NFTs. These data suggest that the nApoECFp17 labeled fragment is being cleaved extracellularly then taken up by microglia. The amino terminal end of apoE4 includes the low-density lipoprotein (LDL) binding domain for full-length apoE because the receptor binding region of apoE is 134-151 [15, 19]. The preferential interaction of apoE4 to the LDL receptor is due to the arginine at position 112 [44], however the low-density lipoprotein receptor protein (LRP) in the same family as the LDL receptor and undergoes rapid and constitutive endocytosis. LRP has been suggested to mediate the neuronal uptake of cholesterol and other lipids including apoE. The amino-terminal fragment produced following cleavage at position D151 may interact with the low-density LRP binding region and be taken up by microglia through receptor mediated endocytosis and

trafficked to the nucleus. The function of this fragment in nucleus of microglia requires further research, but one possible role could be to alter gene expression.

The final important result from these experiments is that collagenases and MMPs are potential proteases capable of cleaving apoE4 or E3. Although the preferential proteolysis of apoE4 versus E3 and E2 has been well documented, the exact nature of the protease(s) involved in this process has not been definitively identified. In our hands, MMP-1 and collagenase produced high-molecular weight complexes *in vitro* following incubation with recombinant apoE4 that were identified following Western blot analysis with nApoECFp17. Similar experiments utilizing active MMP-9 were of particular interest because it produced the predicted ~17 kDa fragment recognized by nApoECFp17 following Western blot analysis. Additionally, in the AD brain, nApoECFp17-labeled nuclei of microglia were identified in the same areas of the extracellular MMP-9 labeling (in plaque-rich regions), which is consistent with where microglia are typically found. These data support previous findings showing increased extracellular levels of MMP-9 in AD [38] and the breakdown and loss of the integrity of the blood-brain barrier associated with AD [45].

Together, the results from my thesis suggest a novel role for an amino-terminal fragment found in the AD brain. The work from my thesis sets up the stage for further research into the mechanism by which apoE4 fragments may be affecting AD pathogenesis. The novel finding of the nApoECFp17 labeled amino-terminal fragment localizing in the nuclei of microglia offers opportunities to study how this fragment may be affecting gene expression. Currently, our lab is continuing to analyze how this fragment is internalized through the LRP or LDL receptors using a microglial cell line.

Since full-length apoE4 has been thought to traffic to the nucleus and up or down regulate various gene expression such as genes associated with apoptosis, pro-inflammatory cytokines, and microtubule assembly [46], analysis of RNA sequence data may shed light into how this fragment affects either signaling pathways or the *APOE4* gene itself. The heightened risk associated with inheritance of the *APOE4* allele has been hypothesized to stem from the susceptibility of apoE4 to proteolysis more than the E3 or E2 forms. Moreover, the enhanced susceptibility of apoE4 to proteolysis suggests apoE4 loses function or gains toxic functions that contribute to AD pathology, but mechanistically remain unexplained. By understanding proteases that are involved in the cleavage of apoE4 and how the resulting fragments affect cells in the brain, it could ultimately be determined how the fragments affect cell signaling pathways or gene expression and establish the role of apoE4 in late-onset AD pathology.

Apolipoprotein E4 Sequence
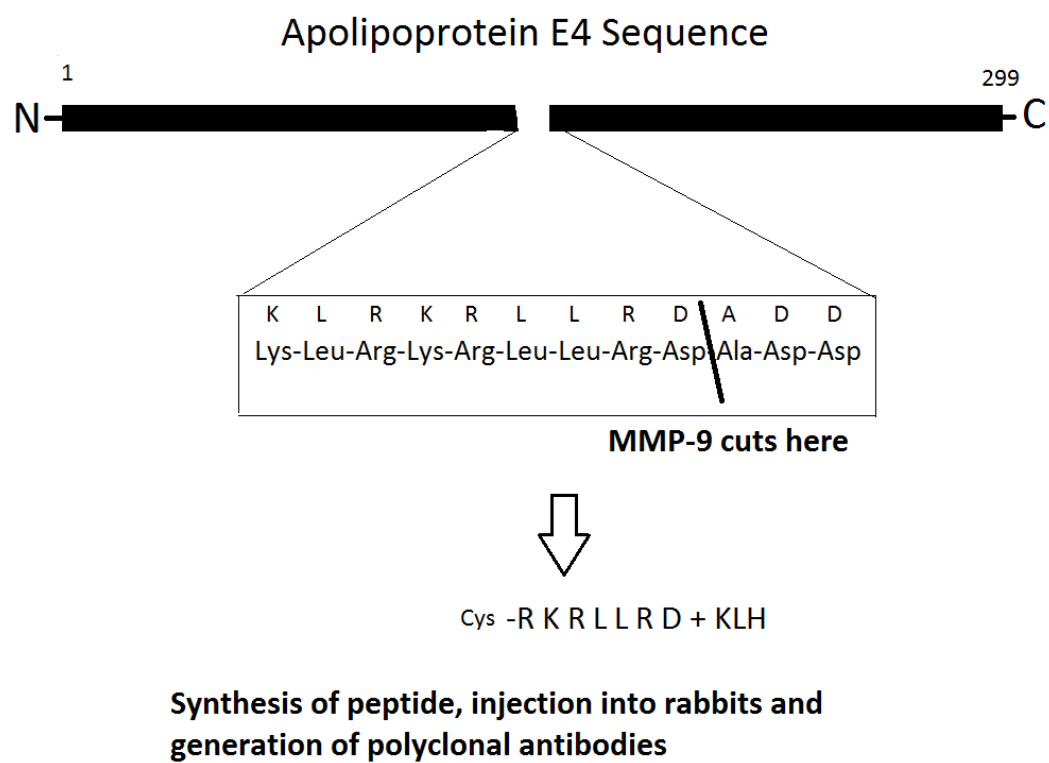
**Figure 1:** **Synthesis of the nApoECFp17 antibody**
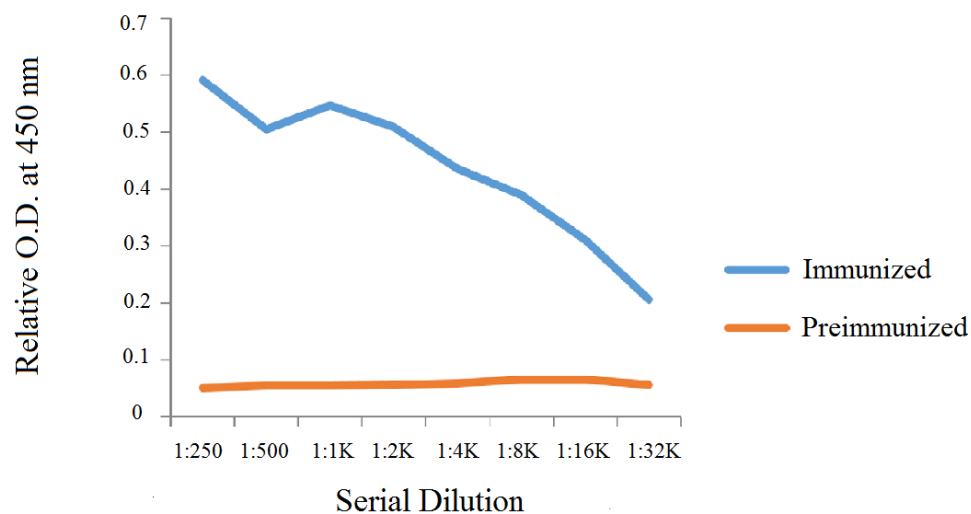
Figure 2: **ELISA: Verification of the polyclonal site-directed cleavage antibody ApoE4 titers in immunized rabbits.** Pre-immune rabbit serum (red line) measured at an absorbance of 450 nm at dilutions from 1:250-1:32,000. And the immunized rabbit serum (blue line) confirms the high titer of n ApoECFp17 antibody in sera from immunized rabbits.
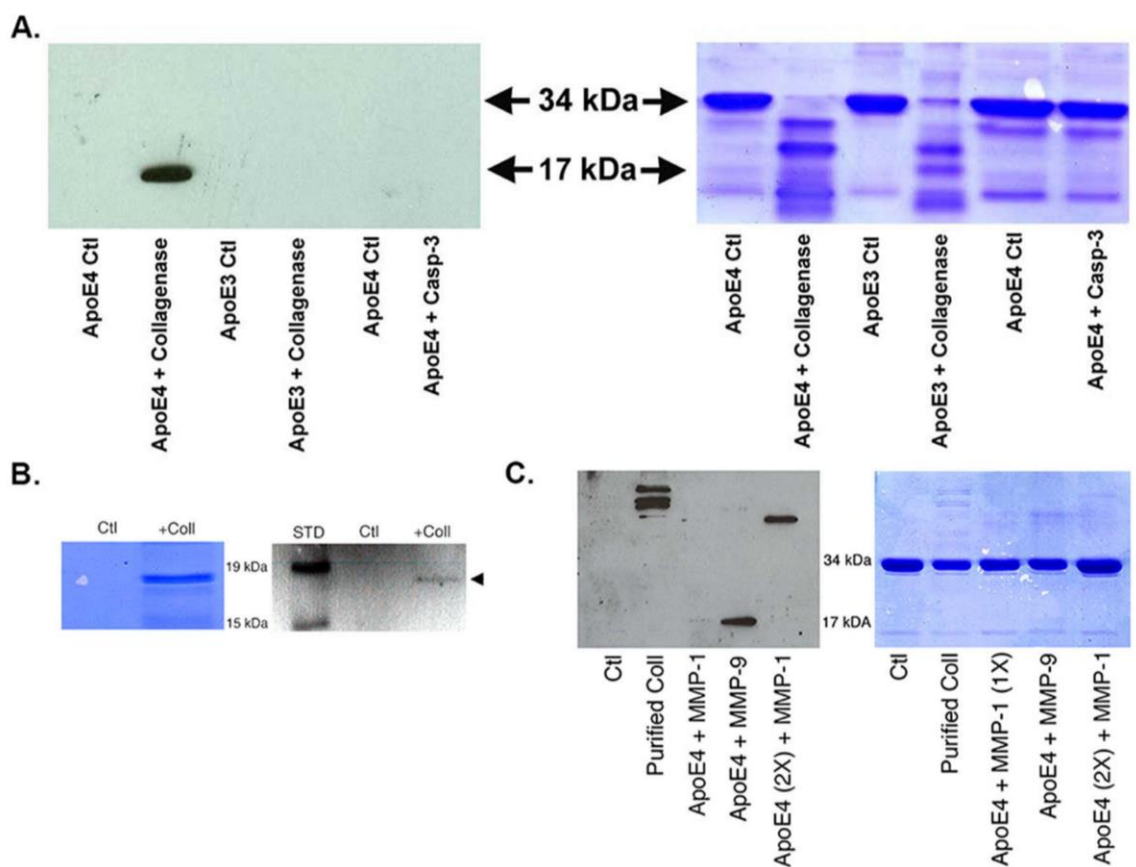
Figure 3: **Characterization of a novel site-directed cleavage antibody to fragmented apoE4. (A):** Preincubation of human recombinant apoE4 but not apoE3 with Type I collagenase for 1.5 hours at 37°C results in the generation of a 17 kDa fragment recognized by affinity-purified nApoECFp17 antibody (lane 2) following Western blot analysis. The right panel depicts the transferred gel slab that was stained with Coomassie blue revealing full-length apoE4 and E3 (34 kDa) as well as the associated fragmentation pattern following incubation with Type I collagenase. **(B):** Immunoprecipitation experiment with the nApoECFp17 antibody following incubation of full-length apoE4 with Type I collagenase revealed the presence of a ~17 kDa band on a Coomassie gel (left panel) that resulted in an immunoreactive band by Western blot using an animo-terminal specific antibody to apoE4 (arrowhead, right panel). **(C)** Identical experiments as in Panel A with the exception that purified collagenase (lane 2), MMP-1 (lanes 3 and 5), or MMP-9 (lane 4) were incubated with recombinant apoE4 (see methods and materials for details). Incubation of apoE4 with either purified collagenase as well as MMP-1 resulted in the presence of high-molecular weight bands detected by nApoECFp17 following Western blot analysis, while incubation of MMP-9 resulted in the detection of a 17 kDa band similar to that generated by Type I collagenase. MMP-1 generated a detectable band only when the apoE4 concentration was doubled (compare lanes 3 vs. 5). In both A and C note the specificity of the nApoECFp17 for cleaved fragments of apoE4 while no reactivity to full-length apoE was observed.
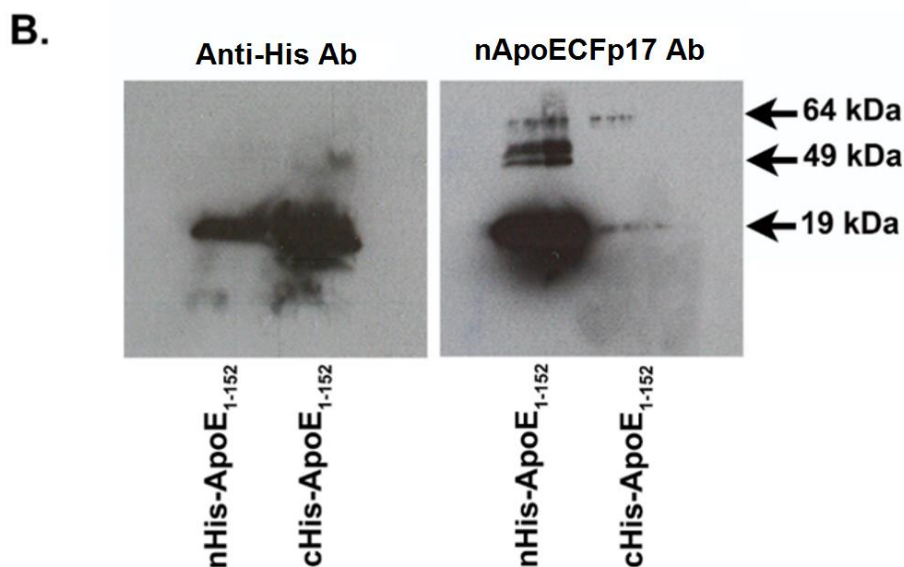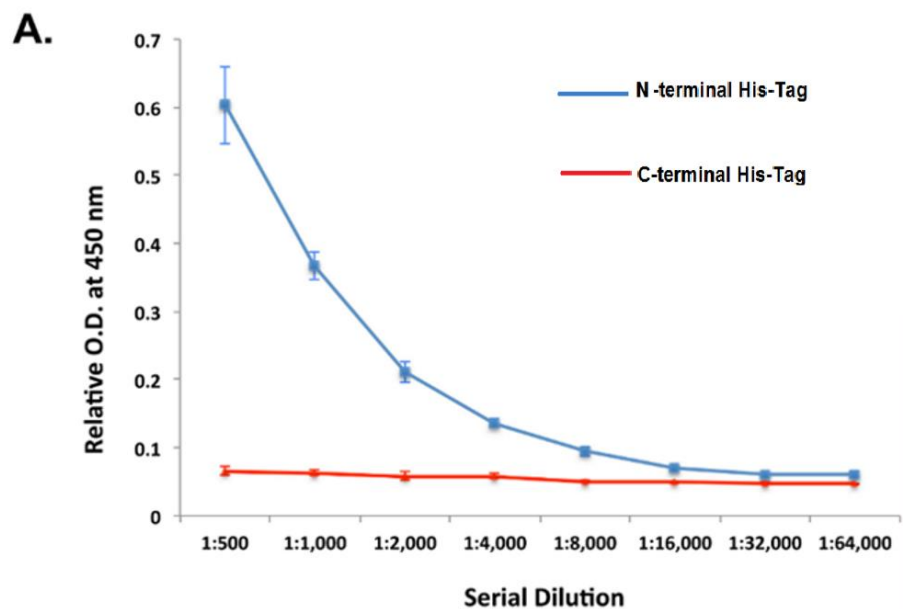
Figure 4: **Specificity of nApoECFp17 to the amino terminal of ApoE 1-151. (A)** ELISA assays in which 96-well plates were coated overnight at 4°C with either ApoE4$_{1-151}$ with the His tag attached to the C-terminal end (red line), or with the His tag attached to the N-terminal end (blue line). The results indicated that the nApoECFp17 antibody only recognized ApoE51-151 in which the His tag was attached to the N-terminal end. **(B)** Similar experiments as in Panel A were performed using Western blot analysis. In this case, the nApoECFp17 antibody preferentially immunolabeled the apoE4 fragment in which the His-tag was localized to the amino-terminal end (Right panel). The left panel shows the identical experiment in utilizing an anti-His antibody that easily labeled both protein fragments regardless of the location of the His tag.
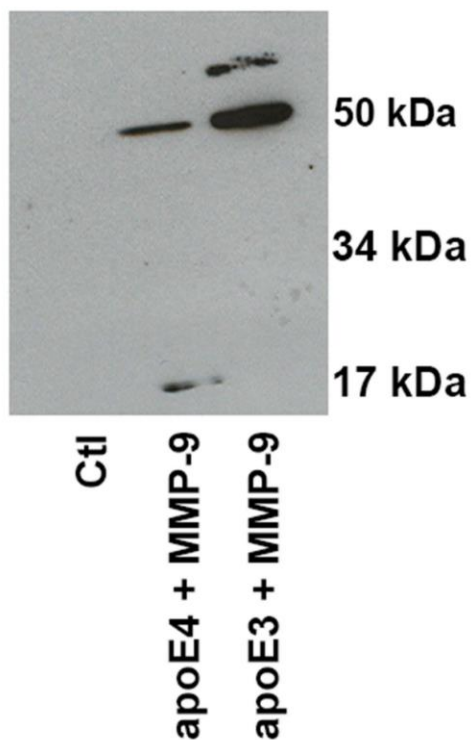
Figure 5:   **Incubation of apoE3 with MMP-9 generates high-molecular weight bands**. Full-length recombinant apoE3 or apoE4 was incubated with activated MMP-9 for 24 hours at 37° C and reactions were terminated by the addition of 5X sample buffer. Protein samples were separated on 15% SDS-PAGE gels, transferred to nitrocellulose, and the probed with the nApoECFp17 antibody overnight at 1:500. The Ctl lane is full length apoE3 protein incubated in the absence of MMP-9.
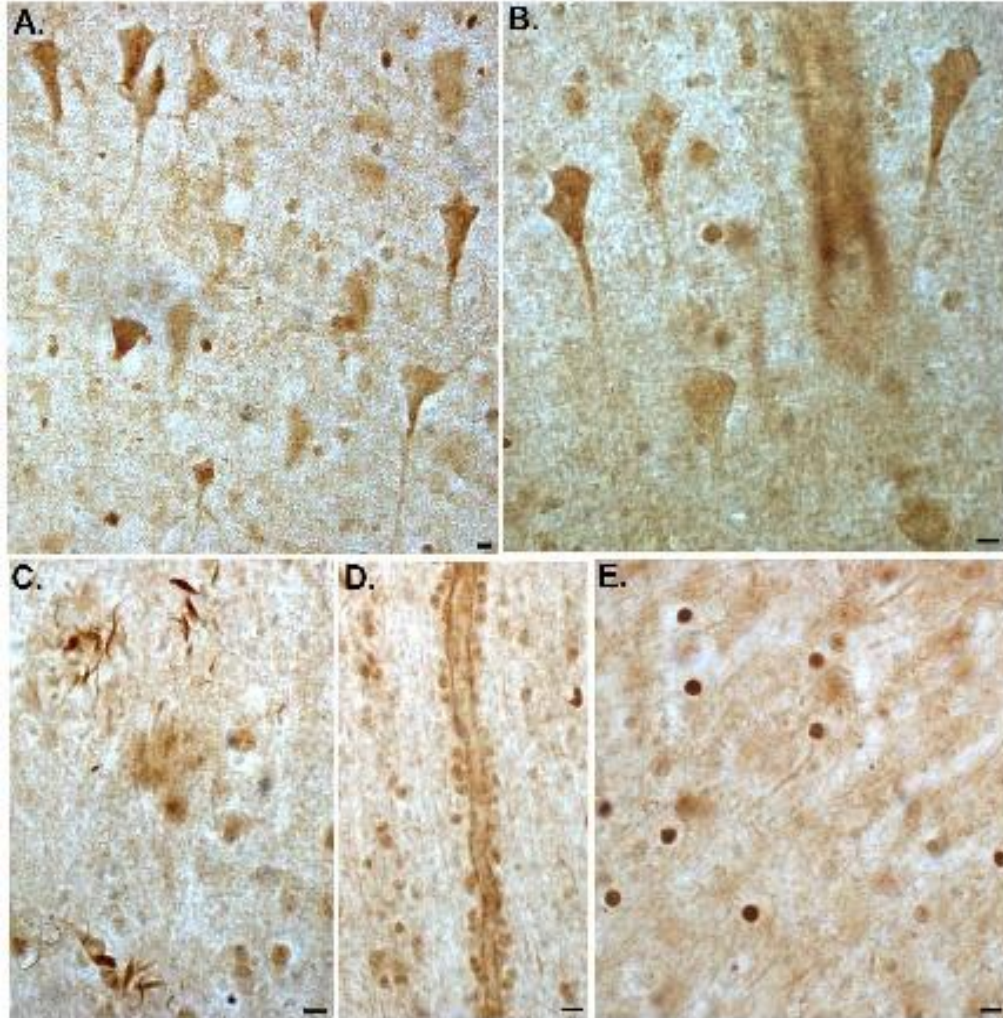
Figure 6: **Detection of fragmented apoE in the frontal cortex of the Alzheimer's disease brain.** Representation bright-field staining in AD frontal cortex tissue sections following application of the nApoeCFp17 antibody. Low **(A)** and high **(B)** magnification of neurons llustrate the apparent loss of cell body integrity in the majority of neurons labeled with the nApoECFp17 antibody. Staining was also observed in neuropil threads within plaque-rich regions **(C)**, along blood vesses (**D**), and the strongest labeling was within small circular structures throughout both gray and white matter **(E)**. All scale bars represent 10 µm.
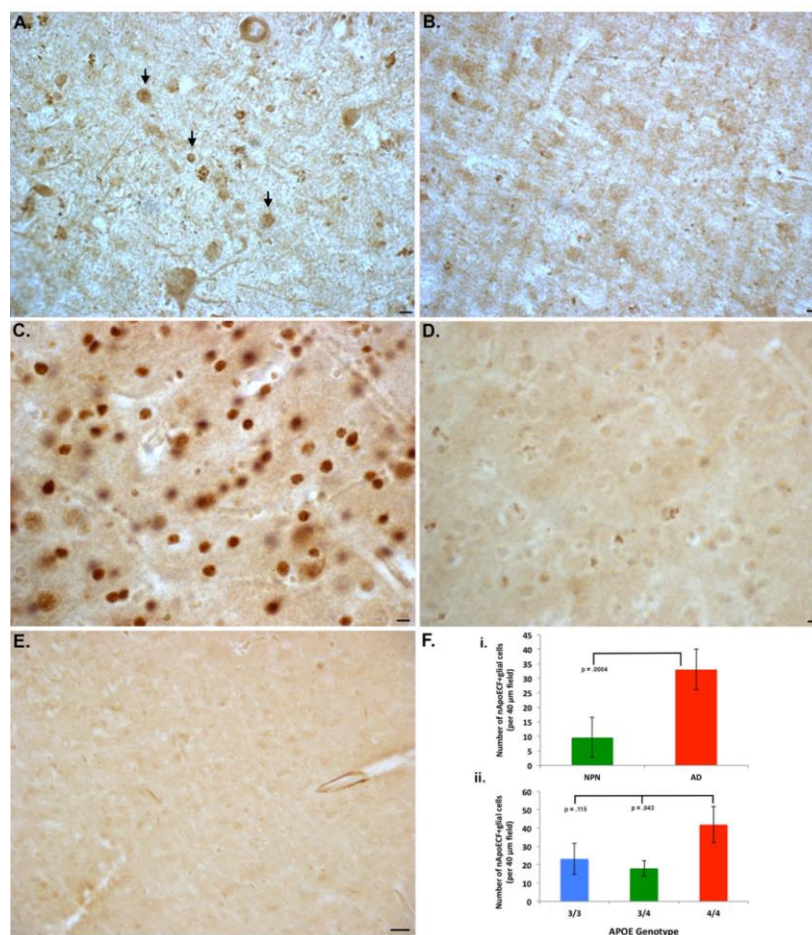
Figure 7: **Specificity of the nApoECFp17 antibody labeling in the Alzheimer's disease brain. (A and B)**: Serial AD frontal cortex sections were immunolabeled with immunized serum **(A)** or preimmune serum **(B)** with specific staining only observed following application of immunized serum. Arrows in Panel A point to stained nuclei following application of immunized serum. **(C and D)**: Serial AD frontal cortex sections were incubated with nApoECFp17 antibody alone **(C)**, or following preadsorption with the peptide used as an immunogen **(D)**. Staining was largely prevented following preadsorption with peptide **(D). (E)**: Relative lack of labeling by nApoECFp17 in a representative neuropathologically normal case**. (F)**: Panel (i) depicts quantitative results of the number of nApoECFp17-labeled nuclei in neuropathologically normal cases (NPN, green bars, N=3) and in AD cases (red bars, N=9) following staining of frontal cortex sections with nApoECFp17. For each case, the number of labeled nuclei was counted in a 40X field (N=3 fields, ±SEM). The data indicated a significant increase in the number of nuclei labeled in AD cases (p= .0004). Panel (ii) illustrates quantitative analysis of the number of nApoECFp17-positive nuclei (per 40 µm field, 3 different fields, ±SEM) in specific *APOE* allele AD cases (N=2). Although higher numbers of nApoECFp17-positive nuclei were observed for the *APOE* 4/4 group as compared to the other genotypes, a significant difference (p<0.5) was only observed following comparison of the *APOE* 4/4 group to 3/4.
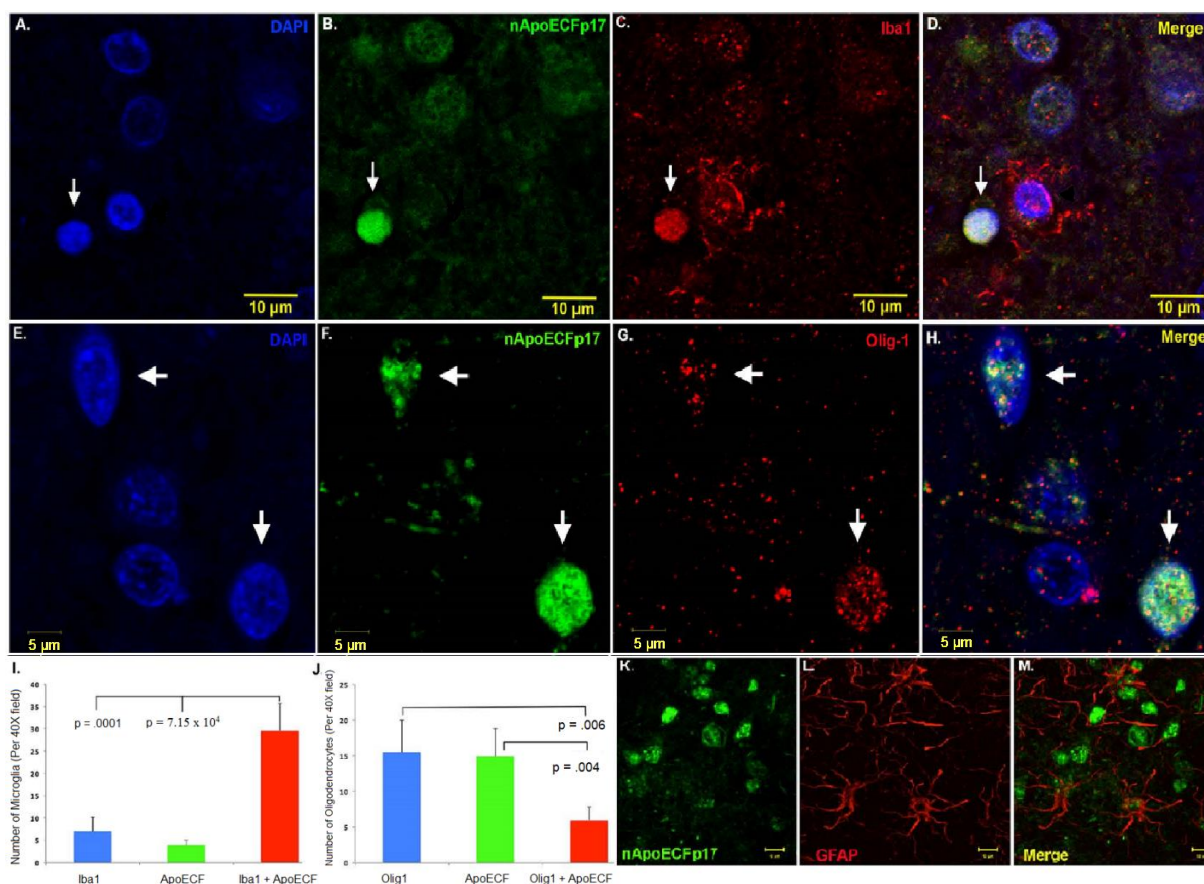
Figure 8: **Nuclear localization of an N-terminal fragment of apoE within microglia of the AD brain**. **(A-D)**: Representative images from confocal immunofluorescence in AD utilizing the nuclear stain, DAPI, **(A)**, nApoECFp17 **(B)**, the microglial specific marker, Iba1 **(C)**, with the overlap image shown in **(D)**. Note the strong nuclear localization of the nApoECFp17 antibody (arrow) within labeled microglia. **(E-H)**: Identical to Panels A-D with the exception that the oligodendrocyte marker, Olig-1, was employed to specifically label oligodendrocytes. **(I-J)**: Quantification of microglia (I) or oligodendrocytes **(J)** double-labeled with nApoECFp17 indicated co-localization in 80% and 27.5% of microglia and oligodendrocytes, respectively. Data show the number of Iba1- or Olig-1-labeled cells alone (blue bars), number of nApoECFp17-labeled nuclei (green bars), and the number of cells with both antibodies (red bars) identified in a 40X field within frontal cortex AD sections by immunofluorescence microscopy (n = 3 fields for 3 different AD cases). **(K-M)**: In contrast to the nuclear localization of nApoECFp17 within microglia and oligodendrocytes, confocal immunofluorescence double-label experiments with nApoECFp17 and the astrocytic marker, GFAP, failed to produce any co-localization between these two markers. Scale bars K-M represent 10 µm.
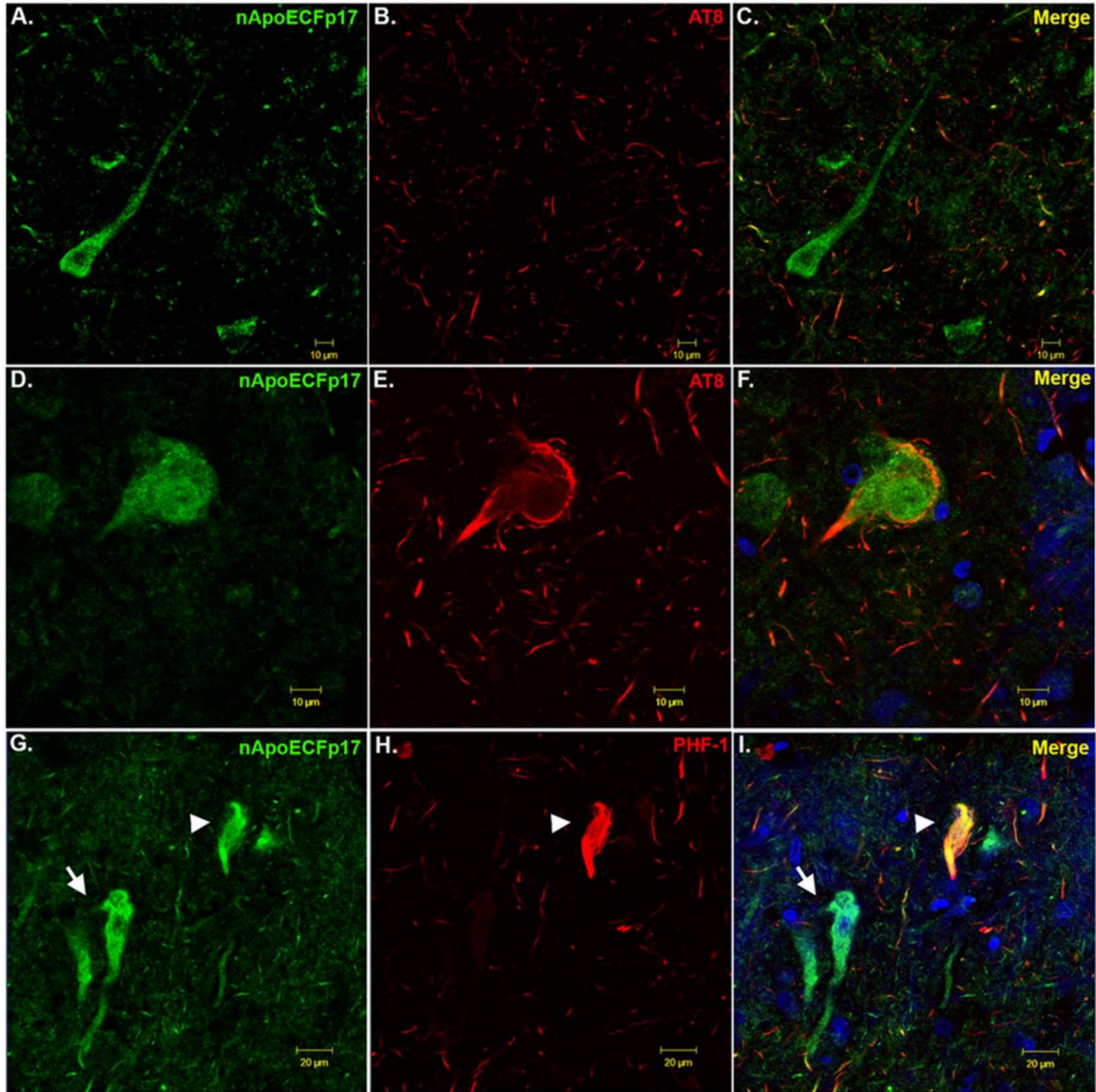
Figure 9: **Localization of an amino-terminal fragment of ApoE within a subset of NFTs of the AD brain**. **(A-F)** Confocal immunofluorescence double-labeling in representative frontal cortex sections of the AD brain utilizing the nApoECFp17 antibody (green), the tangle marker AT8 (red), and the overlap image showed in **(F)**, but not in the majority of neurons labeled with nApoECFp17 **(C)**. **(G-H)** Identical to panels A-F with the exception that the mature tangle marker PHF-1 (red) was used. A subset of fibrillar NFTs showed strong co-localization of the nApoECFp17 and PHF-1 (arrowhead I) in contrast to AT8 labeling. The blue fluorescence in Panels F and I represent the nuclear stain, DAPI.
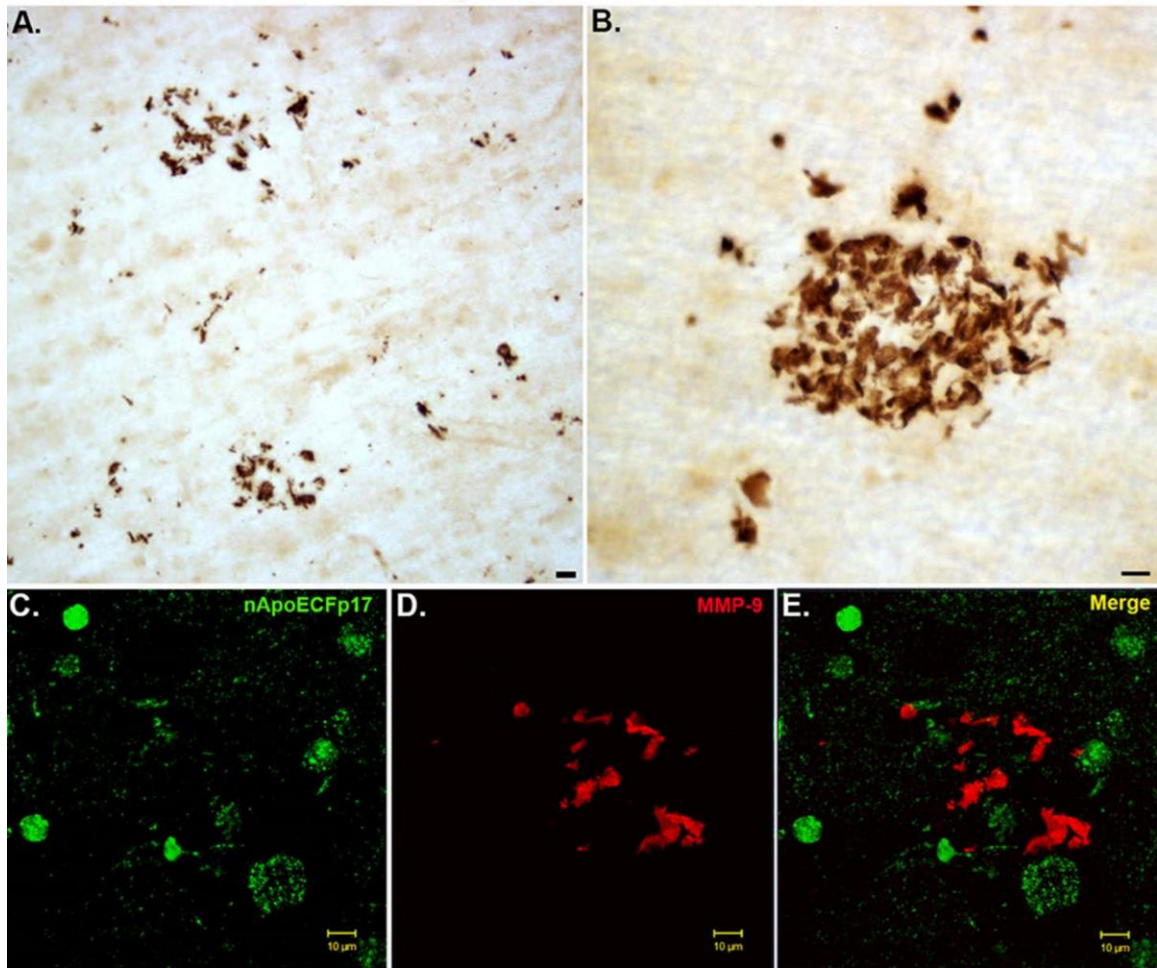
Figure 10: Regional co-localization of extracellular MMP-9 surrounding nApoECFp17 labeled neurons in the AD brain. (A-B) Representative bright field microscopy in AD frontal cortex brain sections in single label experiments utilizing an antibody to MMP-9 labeling gray matter at low magnification (**A**) and high magnification (**B**). Localization appeared to occur in extracellular plaque-rich regions. **(C-E)** Confocal immunofluorescence double-labeling in representative frontal cortex sections of the AD brain utilizing nApoECFp17 (green), MMP-9 (red) reveal regional localization of the two antibodies, but not co-localization in the merged image **(E)**.

TABLES

Table 1:   **Case Demographics**

Group	Age (yrs)	Sex	Cause of death	APOE Genotype
AD	71	M	AD	3/3
AD	61	F	AD	3/4
AD	80	F	Dehydration	4/4
AD	83	F	Cardiac Arrest	3/3
AD	75	F	AD	3/4
AD	65	F	AD	N/A
AD	76	M	AD	3/3
AD	77	F	Cardiac Arrest	N/A
AD	77	F	Sepsis	4/4
NPN	74	F	Cancer	N/A
NPN	65	F	Cardiac Arrest	N/A
NPN	67	F	Heart Failure	N/A

NPN= neuropathologically normal

REFERENCES

1.   Selkoe, D.J., *Alzheimer's disease.* Cold Springs Harbor perspectives in Biology, 2011. **3**(7): p. 1-16.

2.   Selkoe, D.J., *Resolving controversies on the path of Alzheimer's therapeutics.* Nature Medicine, 2011. **17**: p. 1060-1065.

3.   Kang, J., Lemaire, H.G.,Unterbeck, A., Salbaum, J.M., Masters, C.L.,Grzeschik, K.H., *The precursor of Alzheimer's disease amyloid A4 protein resembles a cell-surface receptor.* Nature 1987. **325**(6106): p. 733-6.

4.   Rohn, T.T., *Proteolytic Cleavage of Apolipoprotein E4 as the Keystone for the Heightened Risk Associated with Alzheimer's Disease.* International Journal of Molecular Sciences, 2013. **14**: p. 14908-22.

5.   Alonso, A.C., Zaidi, T., Grundke-Iqbal, I., Iqbal, K., *Role of abnormally phosphorylated tau in the breakdown of microtubules in Alzheimer's disease.* Neurobiology, 1994. **91**: p. 5562-5566.

6.   Kaya, G., et al., *Potential genetic biomarkers in the early diagnosisof Alzheimer disease: APOE and BIN1.* Turkish Journal of Medical Sciences, 2015. **45**: p. 1058-1072.

7.   Kumar, A., et al., *Current and novel therapeutic molecules and targets in Alzheimer's disease.* J Formos Med Assoc, 2016. **115**(1): p. 3-10.

8.   Combs, B., Kneynsberg, A., Kanaan, N.M., *Gene Therapy Models of Alzheimer's Disease and Other Dementias.* Methods Mol Biol, 2016. **1382**: p. 339-66.

9.   Tong, L.M., Fong, H., Huang, Y., *Stem cell therapy for Alzheimer's disease and related disorders: current status and future perspectives.* Exp Mol Med, 2015. **47**: p. e151.

10.   Wang, S., Oelze, B., Schumacher, A., *Age-Specific Genetic Drift in Late-Onset Alzheimer's Disease.* PLoS ONE, 2008. **3**(7).

11.   Herbet, L.E., Weuve, J., Scherr, P.A., Evans D.A., *Alzheimer disease in the United States (2010-2050) estimated using the 2010 census.* Neurology, 2013(80): p. 1778-1783.

12.   Takahashi K., R.C.D., Neumann H., *Clearance of apoptotic neurons without inflammation by microglial triggering receptor expressed on myeloid cells-2.* Exp. Med., 2005(201): p. 647-657.

13.   Mahley, R.W.,Weisgraber, K.H., Huang, Y., *Apolipoprotein E4: A causative factor and therapuetic target in neruopathology, including Alzheimer's disease.* Proc. Natl. Acad. Sci., 2006(103): p. 5644-5651.

14.   Wetterau, J.R., Rall, A.L., Weisgraber, K.H., *Human apolipoprotein E3 in aqueous solution is evidence for two structural domains.* J. Biol. Chem, 1988(263): p. 6240-6248.

15.   Xu, Q., Bernardo, A.,Walker, D., Kanegawa, T., Mahley, R.W., Huang, Y., *Profile and regulation of apolipoprotein E expression in the CNS in mice with targeting of green fluorescent protein gene to the ApoE locus.* J. Neuroscience, 2006(26): p. 4985-4994.

16.   Michikawa, M., Fan, Q., Isobe I., Yanagisawa, K., *Apolipoprotein E exhibits isoform-specfic promotion of lipid efflux from astrocytes and neurons in culture.* J. Neurochem., 2000(74): p. 1008-1016.

17.   Pfrieger, F.W., *Cholesterol homeostasis and function in neurons of the central nervous system.* Cell. Mol. Life Sci, 2003. **60**: p. 1158-171.

18.   Mauch D.H., Nagker, K., Schumacher, S., Goritz, C., *CNS synaptogenesis promoted by glia-derived cholesterol.* Science, 2001(294): p. 1354-1357.

19. Harris, F.M., Brecht,W.J., Xu, Q., et al., *Carboxyl-terminal-truncated apolipoprotein E4 causes Alzheimer's disease-like neruodegeneration and behavioral deficits in transgenic mice.* Proc. Natl. Acad. Sci., 2003(100): p. 10966-10971.

20. Elliot, D.A., Kayan, T., Holinkova, S., et al., *Isoform-specfic proteolysis of apolipoprotein-E in the brain.* Neurobiology Aging, 2011. **32**(2): p. 257-271.

21. Brecht, W.J., Harris, F.M., Chang, S., Tesseur, I., et al. , *Neuron-specific apolipoprotein E4 proteolysis is associated with increased tau phosphorylation in brains of transgenic mice.* J. Neuroscience, 2004. **24**(10): p. 2527-2534.

22. Huang, Y., Liu, X.Q., Wyss-Coray, T., Brecht, W.J., Sanan, D.A., Mahley, R.W., *Apolipoprotein E fragments present in Alzheimer's Disease brains induce neruofibrilary tangle-like intracellular inclusions in neurons.* Proc. Natl. Acad. Sci., 2001. **98**(15): p. 8838-8843.

23. Rohn, T.T., Catlin, L.W., Coonse, K.G., Habig, J.W., *Identification of an animo-terminal fragment of apolipoprotein E4 that localizes to neurofibrillary tangles of the Alzheimer's disease brain.* Brain Res., 2012. **1475**: p. 106-115.

24. Harris, F.M., Tesseur, I., Brecht, W.J., Xu, Q., et al., *Astroglial regulation of apolipoprotein E expression in neuronal cells: implication for Alzheimer's disease.* J. Biol. Chem, 2004(279): p. 3862-3868.

25. Xu, Q., Bernardo, A., Walker, D., Kanegawa, T., Mahley, R.W., Huang Y., *Profile and regulation of apolipoprotein E expression in the CNS in mice with targting of green fluorescent protein gene to the ApoE locus.* j. Neuroscience, 2006. **26**(19): p. 4985-4994.

26. Poirier, J.,Miron, J., Picard, C., Gormley, P., et al., *Apolipoprotein E represents a potent gene based therapeutic target for the treatment of sporadic Alzheimer's disease.* Alzheimer's Dement., 2008(4): p. 91-97.

27. Poirier, J., *Apolipoprotein E, cholesterol transport and synthesis in sporadic Alzheimer's disease.* Neurobiol. Aging., 2005(26): p. 355-361.

28. Wisniewski, T., Frangione, B., *Apolipoprotein E: a patholigcal chaperone protein in patients with cerebral and systemic amyloid.* Neurosci. Lett., 1992(135): p. 235-238.

29. Aleshkov, S., Abraham, C.R., and Zannis, V.I., *Interaction of nascent ApoE2,ApoE3, and ApoE4 isofrms expressed in mammalian cells with amyloid peptide beta (1-40). Relevance to Alzheimer's disease.* Biochemistry, 1997(36): p. 10571-10580.

30. Tokuda, T., Calero, M., Matsubara, E., Vidal, R., Kumar A., et al., *Lipidation of apolipoprotein E influences its isoform-specific interaction with Alzheimer's amyloid beta peptides. .* Biochem. J. , 2000(348): p. 359-365.

31. Bien-Ly N., Andrews-Zwilling, Y., Xu, Q., Bernardo, A., Wang, C. Huang, Y., *C-terminal-truncated apolipoprotein E4 inefficiently clears amyloid beta and acts in concert with Abeta to elicit neuronal and behavioral deficits in mice.* Proc. Natl. Acad. Sci., 2011. **108**(10): p. 4236-4241.

32. Tiraboschi, P., Hansen, L.A., Masliah, E., Alford, M., et al., *Impact of APOE genotype on neuropathologic and neuro-chemical markers of Alzheimer disease.* Neurology, 2004(62): p. 1977-1983.

33. Sunderland, T., Mirza, N., Putnam, K.T., Linker, G., et al., *Cerebrospinal fluid beta-amyloid 1-42and tau in control subjects at risk for Alzheimer's disease: the effect of APOE epsilon4 allele.* Biol. Psychiatry, 2004(56): p. 670-676.

34. Chang, S., Ran Ma, T., Miranda R.D., Balestra, M.E., Mahley, R.W., Huang, Y., *Lipid-and receptor-binding regions of apolipoprotein E4 fragments act in concert to cause mitochondrial dysfunction and neurotoxicity.* Proc. Natl. Acad. Sci., 2005. **102**(51): p. 18694-9.

35. Andrews-Zwilling, Y., Bien-Ly, N.,Xu, Q., Li, G., Bernardo, A., Yoon, S.Y., et al., *Apolipoprotein E4 causes age-and tau-dependents impairment of GABAergic*

interneurons, leading to learning and memory deficits in mice. J. Neuroscience, 2010. **30**(41): p. 13707-17.

36. Strittmatter W.J., S., A.M., Goedert, M., Weisgraber, K.H., Dong, L.M., Jakes, R., Huang, D.Y., Pericak-Vance, M., Schmechel, D., Roses, A.D., *Isoform- specific interactions of apolipoprotein E with microtubule-associated protein tau: implications for Alzheimer's disease.* Proc. Natl. Acad. Sci., 1994. **91**(23): p. 11183-6.

37. Nakamura, T., Watanabe, A., Fujino, T., Hosono, T., Michikawa, M., *Apolipoprotein E4 (1-272) fragment is associated with mitochondrial proteins and affects mitochondrial function in neruonal cells.* Mol. Neurodegener., 2009(4): p. 35.

38. Dafnis, I., Stratikos, E., Tzinia, A., Tsilibary, T.C., Zannis, V.I., Chroni, A., *An apolipoprotein E4 fragment can promote intracellular accumulation of amyloid peptide beta 42.* J Neurochem., 2010. **115**(4): p. 873-884.

39. Zhou, W., Scott, S.A., Shelton, S.B., Crutcher, K.A., *Cathepsin D-mediated proteolysis of apolipoprotein E: possible role in Alzheimer's disease.* Neuroscience, 2006(143): p. 689-701.

40. Marques, M.A., Owens, P.A., Crutcher, K.A., *Progress toward identification of protease activity involved in proteolysis of apolipoprotein e in human brain.* J. Mol. Neuroscience, 2004(24): p. 73-80.

41. Gottschall, P.E., Deb, S., *Regulation of matrix metalloproteinase expression in astrocytes, microglia and neruon.* Neurorimmunomodulation, 1996(3): p. 69-75.

42. Candelario-Jalil, E., Yang, Y., Rosenberg, G.A., *Diverse roles of matrix metalloproteinases and tissue inhibitors of metalloproteinases in neuroinflammation and cerebral ischemia.* Neuroscience, 2009. **158**: p. 983-994.

43. Egensperger, R., Kosel, S., Eitzen, V.U., Graeber, M.B., *Microglial activation in Alzheimer disease: Association with APOE genotype.* Brain Pathol., 1998(8): p. 439-447.

44. Weisgraber, K.H., Mahley, R.W., *Human apolipoprotein E: the Alzhimer's disease connection.* FASEB, 1996. **10**: p. 1485-.

45. Bell, R.D., et al. , *Apolipoprotein E controls cerebrovascular integrity via cyclophilin A.* Nature, 2012. **485**(7399): p. 512-516

46. Theendakara, V., Peters-Libeu, C.A., Spilman, P., Poksay, K.S., Bredesen, D.E., Rao, R.V., *Direct Transcriptional Effects of Apolipoprotein E.* J. Neuroscience, 2016. **36**(3): p. 685-700.